



# Microbes vs. chemistry in the origin of the anaerobic gut lumen

Elliot S. Friedman<sup>a</sup>, Kyle Bittinger<sup>b</sup>, Tatiana V. Esipova<sup>c</sup>, Likai Hou<sup>d,1</sup>, Lillian Chau<sup>a</sup>, Jack Jiang<sup>a</sup>, Clementina Mesaros<sup>e</sup>, Peder J. Lund<sup>c,f</sup>, Xue Liang<sup>g,2</sup>, Garret A. FitzGerald<sup>g</sup>, Mark Goulian<sup>h</sup>, Daeyeon Lee<sup>d</sup>, Benjamin A. Garcia<sup>c,f</sup>, Ian A. Blair<sup>e</sup>, Sergei A. Vinogradov<sup>c,i,3</sup>, and Gary D. Wu<sup>a,3</sup>

<sup>a</sup>Division of Gastroenterology, Perelman School of Medicine, University of Pennsylvania, Philadelphia, PA 19104; <sup>b</sup>Division of Gastroenterology, Hepatology, and Nutrition, Children's Hospital of Philadelphia, Philadelphia, PA 19104; <sup>c</sup>Department of Biochemistry and Biophysics, Perelman School of Medicine, University of Pennsylvania, Philadelphia, PA 19104; <sup>d</sup>Department of Chemical and Biomolecular Engineering, Perelman School of Medicine, University of Pennsylvania, Philadelphia, PA 19104; <sup>e</sup>Institute for Translational Medicine and Therapeutics, Perelman School of Medicine, University of Pennsylvania, Philadelphia, PA 19104; <sup>f</sup>Penn Epigenetics Institute, Perelman School of Medicine, University of Pennsylvania, Philadelphia, PA 19104; <sup>g</sup>Department of Systems Pharmacology and Translational Therapeutics, Perelman School of Medicine, University of Pennsylvania, Philadelphia, PA 19104; <sup>h</sup>Department of Biology, School of Arts and Sciences, University of Pennsylvania, Philadelphia, PA 19104; and <sup>i</sup>Department of Chemistry, School of Arts and Sciences, University of Pennsylvania, Philadelphia, PA 19104

Edited by Lora V. Hooper, The University of Texas Southwestern, Dallas, TX, and approved March 9, 2018 (received for review October 26, 2017)

**The succession from aerobic and facultative anaerobic bacteria to obligate anaerobes in the infant gut along with the differences between the compositions of the mucosally adherent vs. luminal microbiota suggests that the gut microbes consume oxygen, which diffuses into the lumen from the intestinal tissue, maintaining the lumen in a deeply anaerobic state. Remarkably, measurements of luminal oxygen levels show nearly identical pO<sub>2</sub> (partial pressure of oxygen) profiles in conventional and germ-free mice, pointing to the existence of oxygen consumption mechanisms other than microbial respiration. In vitro experiments confirmed that the luminal contents of germ-free mice are able to chemically consume oxygen (e.g., via lipid oxidation reactions), although at rates significantly lower than those observed in the case of conventionally housed mice. For conventional mice, we also show that the taxonomic composition of the gut microbiota adherent to the gut mucosa and in the lumen throughout the length of the gut correlates with oxygen levels. At the same time, an increase in the biomass of the gut microbiota provides an explanation for the reduction of luminal oxygen in the distal vs. proximal gut. These results demonstrate how oxygen from the mammalian host is used by the gut microbiota, while both the microbes and the oxidative chemical reactions regulate luminal oxygen levels, shaping the composition of the microbial community throughout different regions of the gut.**

microbial ecology | gut microbiota | luminal oxygen | phosphorescence quenching | oxygen probes

The composition of the gut microbiota is spatially segregated along the length of the gut as well as radially, whereby many factors, including those determined purely by the host physiology, create a multitude of microenvironments (1, 2). The factors influencing microbial distribution along the length include glandular secretions (i.e., gastric acid, bile, and pancreatic fluids), structural differences between the small and large intestine, motility patterns, and epithelial antimicrobial peptide secretion. However, much less is known about the radial distribution of the gut microbiota. Mucus produced by the intestinal epithelium plays an important role in shaping the mucosally adherent gut microbiota that has glycan-foraging properties (3–5) and responds to both antimicrobial peptides (6) and mucosally secreted IgA (7, 8).

Diffusion of molecular oxygen from the intestinal tissue into the gut lumen has also been assumed to play a role in shaping the microbial composition (9). It is known that the gut microbiota undergoes transformation from aerobic and facultatively anaerobic bacteria to obligate anaerobes early in life. This succession is consistent with a hypothesized transition to an anaerobic environment due to the rapid consumption of oxygen by aerotolerant organisms. Previously, we found that the radial distribution of the gut microbiota correlates with the oxygen concentration gradient, where there is a higher representation of aerotolerant

bacteria adherent to the mucosa—that is, in the vicinity of the relatively well-oxygenated intestinal tissue relative to the anaerobic lumen (10). Alterations in the composition of the gut microbiota observed upon hyperbaric oxygen treatment provided additional support for the notion that the microbial distribution is highly sensitive to the oxygen in the environment (10). Nevertheless, several observations about the composition and function of the gut microbiota remain unexplained, including the dominance of facultative anaerobic organisms such as *Streptococci spp.* in the small intestine (11), as well as the fact that it is possible to colonize germ-free mice with obligate anaerobic bacteria (5). Indeed, if the gut lumen would be maintained in the anaerobic state solely by oxygen-consuming bacteria, the gut of the germ-free animals would have the same oxygen concentration as the surrounding intestinal tissue, and the obligate anaerobes would not be able to survive in such an environment.

In this study, we used the phosphorescence quenching method in combination with well-established tissue oxygen probe Oxyphor G4 (12) to quantify oxygen levels in intestinal tissue, while a newly developed microsphere-based probe Oxyphor MicroS was used to measure oxygen in the gut lumen. We correlated the measured levels with the composition of the mucosally adherent

## Significance

**It is generally thought that the gut microbes consume oxygen and maintain the lumen in a deeply anaerobic state. However, we found that the gut of germ-free mice is also deeply anaerobic, suggesting that there exist other mechanisms responsible for oxygen consumption in addition to the microbes' respiration. These mechanisms comprise oxidative reactions, such as the oxidation of lipids and other organic substrates. Both the microbiota and the oxidative chemistry regulate luminal oxygen levels that in turn influence the composition of the microbial communities throughout the intestinal tract.**

Author contributions: M.G., S.A.V., and G.D.W. designed research; E.S.F., K.B., T.V.E., L.H., L.C., J.J., C.M., P.J.L., X.L., and S.A.V. performed research; L.H. and D.L. contributed new reagents/analytic tools; E.S.F., K.B., C.M., P.J.L., X.L., G.A.F., M.G., B.A.G., I.A.B., S.A.V., and G.D.W. analyzed data; and E.S.F., C.M., P.J.L., M.G., S.A.V., and G.D.W. wrote the paper.

The authors declare no conflict of interest.

This article is a PNAS Direct Submission.

Published under the PNAS license.

<sup>1</sup>Present address: School of Mechatronics Engineering, Harbin Institute of Technology, 150001 Harbin, China.

<sup>2</sup>Present address: Merck Exploratory Science Center, Cambridge, MA 02141.

<sup>3</sup>To whom correspondence may be addressed. Email: vinograd@penmedicine.upenn.edu or gdwu@penmedicine.upenn.edu.

This article contains supporting information online at [www.pnas.org/lookup/suppl/doi:10.1073/pnas.1718635115/-DCSupplemental](http://www.pnas.org/lookup/suppl/doi:10.1073/pnas.1718635115/-DCSupplemental).

Published online April 2, 2018.

and luminal microbiota along the length of the intestinal tract of both conventionally housed and germ-free mice. Remarkably, luminal oxygen levels were found to be nearly indistinguishable between conventionally housed and germ-free mice, being close to zero in the cecum in both cases. This observation suggests that in addition to the respiration by aerotolerant microorganisms, there exist other efficient mechanisms by which oxygen is consumed in the gut, such as oxygen-consuming chemical reactions. The rates of these processes, however, are substantially lower than oxygen consumption by the luminal contents of conventional germ-containing mice. Nevertheless, these alternative mechanisms may play a pivotal role in establishing the composition of the microbiota at early stages of life. Furthermore, their presence opens up a range of possibilities for altering the existing gut microbiota (e.g., by providing additional control over microbial recolonization in clinical setting).

Second, oxygen levels in the lumen of the proximal small intestine (e.g., stomach and duodenum) were found to be much greater than in the distal small intestine (terminal ileum), and the oxygen levels in the latter were still higher than in the cecum, where oxygen was practically undetectable (10). Correlation between these levels and both the composition and biomass of the mucosally adherent and luminal microbiota suggests that the microbiota responds to oxygen, possibly in a manner that is dependent upon the mucosal surface area in each intestinal segment.

Overall, luminal oxygenation along the length of the mammalian gut is nonuniform and is likely to be a function of the biomass of the gut microbiota, the composition of the luminal contents, and possibly the anatomy of the surrounding tissue. The effects of oxygenation on the composition of the local microbial community may be particularly relevant in the proximal small intestine, given the low biomass of the local microbiota and the fact that it is directly exposed to dietary nutrients as well as pancreatico-biliary secretions.

## Results

**Measurements of Oxygen in the Intestinal Tissue and in the Gut Lumen of Mice.** Oxygen concentration measurements were performed using the phosphorescence quenching method as previously described (10). For measurements in the intestinal tissue, a well-established hydrophilic phosphorescent probe Oxyphor G4 (or PdG4) (12) was injected into the tail vein of a mouse, and the phosphorescence was excited locally by a laser focused on the intestinal compartment of interest (stomach, duodenum, cecum, etc.) in a spot  $\sim 0.1$  mm in diameter.

Water-soluble Oxyphors are not appropriate for oxygen measurements in the lumen, where they may interact with luminal contents, undergo unpredictable transformations during digestion, and as a result, lose their ability to report on oxygen quantitatively. To address this issue, we previously developed micrometer-scale phosphorescent particles (10–20  $\mu$ m in diameter), where the phosphorescent dye molecules (Pt tetrabenzoporphyrin) were dissolved in a solid polymer matrix (10). Due to the large micrometer-scale size of the particles (large volume/surface ratio), the immediate environment of nearly all oxygen-sensing chromophores is due to the polymer. Consequently, oxygen response of the particles is largely unaffected by the medium in which these particles are dispersed, whether it is water, more viscous fluid, or semisolid luminal material, ensuring quantitative measurements.

The original phosphorescent microprobes were prepared by grinding solid polymer material, rendering particles with very broad size distribution. The oxygen quenching response of smaller particles ( $<1$   $\mu$ m) likely retained some sensitivity to the environment, making oxygen measurements in the lumen less accurate. To eliminate this ambiguity, here we used a microfluidic technique that allowed us to prepare uniformly spherical particles with exceptionally narrow size distribution ( $32 \pm 2$   $\mu$ m in diameter) (Fig. 1A–C). The microspheres were composed of poly(methyl methacrylate) (PMMA) containing codissolved Pd tetrabenzoporphyrins (12). The oxygen quenching response of

the probes was calibrated, as previously described (10), in water and in substances of varying viscosities, showing minimal dependence on the composition of the media (Fig. 1D). The probes remained intact in the gut lumen after feeding to mice and digestion, as evidenced by imaging of the microspheres recovered from the luminal material (Fig. 1E–G).

**Luminal Oxygen Levels in Germ-Free and Conventionally Housed Mice Are Nearly Identical, with Higher Values in the Proximal Gut and Close to Zero in the Distal Intestine.** The newly developed phosphorescent microspheres (Oxyphor MicroS) were used to quantify intraluminal oxygen levels along the intestinal tract, including stomach, proximal small intestine (duodenum), distal small intestine (terminal ileum), and cecum. In a parallel set of experiments, with the aid of hydrophilic oxygen probe Oxyphor G4 (10), tissue oxygen levels were measured in the same sites.

The most striking finding was that the luminal oxygen levels in germ-free mice are almost the same as in conventionally housed mice in all regions of the intestine. In both germ-free and conventional mice, the luminal oxygen levels were found to be closer to the tissue levels in the stomach and duodenum, but in the lumens of the terminal ileum and cecum, oxygen was near zero (Fig. 2). In the case of conventionally housed mice, low oxygen in the distal gut is consistent with the greater biomass of the microbiota (13), where the aerotolerant microorganisms are capable of consuming oxygen. However, in the case of germ-free animals, a fully anaerobic environment cannot be explained by microbial respiration and, therefore, must originate in other oxygen depletion mechanisms (see below).

Both tissue and luminal oxygen levels were found to be greater in the duodenum than in the stomach. The highly vascularized nature of the duodenum tissue (14) as well as the presence of villi in the small intestine (15) that greatly increase mucosal surface area may facilitate exchange of oxygen between the duodenum tissue and the lumen. However, to our surprise, the luminal oxygen levels in the duodenum were found to be even higher than the tissue levels (Fig. 2A), and this difference was reproducible and highly statistically significant. This result is unexpected and calls for additional investigation. First, it is possible that pancreaticobiliary secretions delivered at high concentrations directly into the duodenum may be more oxygenated than the duodenal tissue, where average oxygen levels are set by the balance between the blood delivery and consumption by the mitochondrial respiration. Second, we cannot entirely exclude the possibility that these secretions might also act as alternative

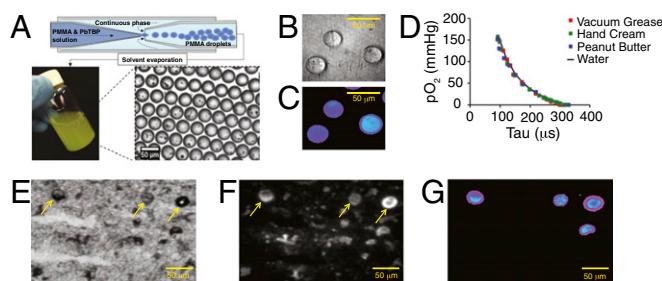


**Fig. 1.** Microsphere-based phosphorescent probe Oxyphor MicroS for quantification of oxygen levels in the gut lumen. (A) Schematic illustration of the process of fabrication of Oxyphor MicroS using a microfluidic device. Wide-field images of the microspheres (B) in transmitted light and (C) phosphorescence in time-gated mode after excitation by a 20  $\mu$ s-long light pulse ( $\lambda_{\text{ex}} = 630$  nm; for imaging setup, see ref. 12). (D) Oxygen calibration plots of Oxyphor MicroS in substances of varying viscosities. Images of samples of murine cecal material after feeding Oxyphor MicroS: (E) transmitted light and (F) integrated luminescence intensity under continuous wave illumination (including back-scattered light and autofluorescence). (G) Phosphorescence in time-gated mode, showing signals only from the microspheres. Arrows indicate the location of Oxyphor MicroS probes (E and F).

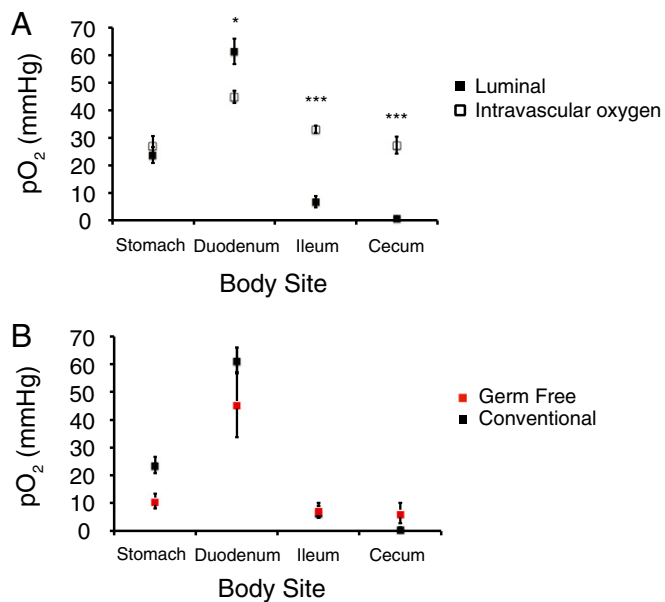


**Fig. 2.** Levels of oxygen in intestinal tissue vs. the lumen throughout the length of the intestinal tract. (A) Oxygen levels in conventionally housed mice. (B) Comparison of luminal oxygen levels throughout the length of the intestinal tract in conventionally housed vs. germ-free mice. For conventionally housed mice (intravascular):  $n = 10$  for stomach,  $n = 10$  for duodenum,  $n = 6$  for ileum, and  $n = 6$  for cecum. For conventionally housed mice (luminal):  $n = 24$  for stomach,  $n = 20$  for duodenum,  $n = 10$  for ileum, and  $n = 13$  for cecum. For germ-free mice:  $n = 3$  for stomach and duodenum,  $n = 9$  for ileum, and  $n = 8$  for cecum. Mean  $\pm$  SEM. \* $P < 0.05$ ; \*\*\* $P < 0.001$  (two-tailed unpaired Student's  $t$  test).

quenchers of the probe phosphorescence, shortening its triplet lifetime and thereby giving an impression of higher oxygen concentration. Although our calibration experiments reveal that the microsphere-embedded probe is virtually insensitive to the properties of the surrounding medium, it is still possible that small-molecule quenchers, possibly present in pancreatic secretions, may affect the probe decay time. Additional studies, perhaps including probes based on larger microparticles as well as quenching experiments involving isolated contents of the duodenum, may clarify this issue.

In the absence of microbes consuming oxygen in the lumen of germ-free mice, one possible mechanism responsible for maintaining the anaerobic state could involve oxygen-involving reactions (e.g., oxidation of the luminal contents). To examine this possibility, we conducted a series of *in vitro* experiments. In a typical run, cecal contents in a vial were dispersed in sterile water containing an oxygen probe (Oxyphor G4) and equilibrated with air at 37 °C ( $pO_2 = 141$  mmHg, water vapor pressure = 47.1 mmHg). The vial was sealed with a cap ensuring that no air bubbles were left in the headspace, and oxygen concentration was monitored over time by measuring the phosphorescence. To ensure sterility of our procedure, several control vials were treated with  $\gamma$ -radiation after sealing, confirming that the protocol was indeed fully sterile.

The cecal contents from germ-free mice gradually consumed oxygen over several hours, ultimately leading to an anaerobic state. As expected, the rate of consumption correlated with the amount of material in the vial (Fig. 3A). Noteworthy are the pronounced exponential-like curvatures of the oxygen depletion plots, indicating that the kinetics of the underlying process(es) is the first (or higher) order in oxygen, thus supporting the notion that the oxidation chemistry is responsible for the consumption of oxygen in germ-free cecal material. The cecal contents from conventionally housed mice were also found to engage in oxygen-consuming processes, however in this case, the rates were

substantially higher (minutes rather than hours), and the oxygen consumption plots were nearly linear (zero order in oxygen) down to very low oxygen pressures ( $<1$  mmHg) (Fig. 3A). To confirm that the presence of oxygen-consuming bacteria was indeed the cause for the rapid consumption of oxygen by the cecal contents of conventionally housed mice, we added the facultative anaerobe *Escherichia coli* to germ-free cecal contents ( $1.25$ – $1.50 \times 10^9$  cfu/g cecal contents). Indeed, this greatly increased the rate of oxygen consumption, resulting in oxygen consumption plots similar to those observed in the case of conventional mice (Fig. S1). Under these conditions, the constant rates of depletion (linear plots) are consistent with respiration being the primary mechanism of oxygen depletion (16). In contrast, the addition of an obligate anaerobe, *Clostridia sordelli* ( $1.75$ – $2.15 \times 10^9$  cfu/g cecal contents), to germ-free cecal contents led to a rate of oxygen consumption that was somewhat faster than that observed for germ-free cecal contents alone but slower than either in the case of conventional cecal contents or germ-free cecal contents with added *E. coli* (Fig. S1). This increased rate of oxygen consumption may reflect the presence of noncytochrome-dependent oxygen scavenging systems such as water-forming NADH oxidases and other oxidoreductases that have been described for obligate anaerobes such as *Clostridia spp.* (17, 18).

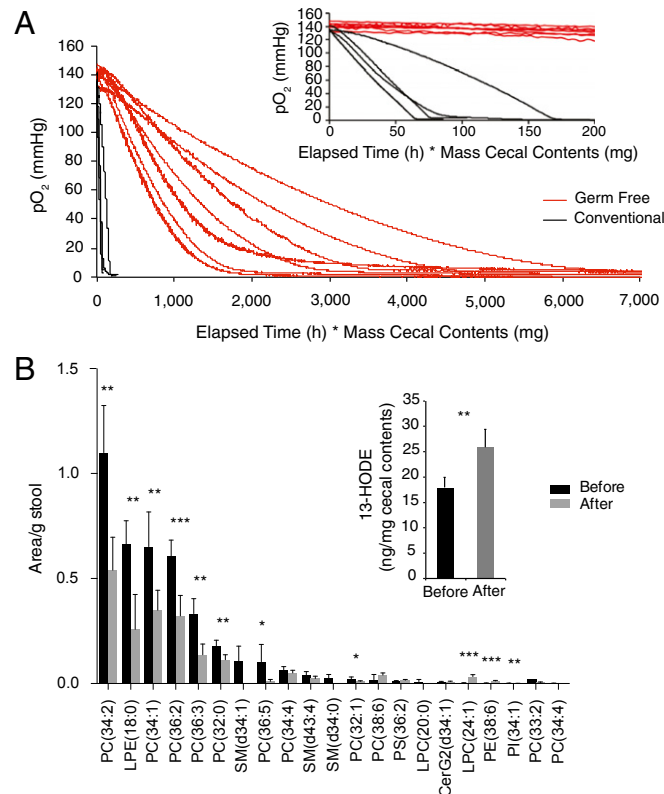


**Fig. 3.** Dynamics of oxygen consumption by cecal contents *in vitro* and the effects of oxygen-involving reactions on the protein and lipid compositions. (A) Oxygen consumption by cecal contents of conventionally housed and germ-free mice. Cecal contents from conventionally housed mice consumed oxygen within 0.3–1 h, while cecal contents from germ-free mice consumed oxygen within 2.5–18 h, depending on the mass of the cecal contents used in these *in vitro* experiments. The x axis (time) is adjusted to account for the mass of the cecal contents: time (h)  $\times$  mass of cecal contents (mg) to facilitate comparison. (B) Results of the lipidomic analysis of germ-free cecal material before and after oxygen consumption as well as the identification of lipid oxidation products (13-HODE) using deuterium-labeled LA (Inset). Mean  $\pm$  SEM. \* $P < 0.01$ ; \*\* $P < 0.01$ ; \*\*\* $P < 0.001$ . Two-tailed Student's  $t$  test (unpaired, main figure; paired, Inset).

Thus, we conclude that chemical reactions maintain the distal gut of germ-free mice in a deeply anaerobic state, a finding that may have particular relevance to the initial development of the infant gut microbiota.

**Mass-Spectrometric Analysis of Cecal Contents Exposed to Oxygen Suggests That Lipid Oxidation May Be One of the Processes Responsible for Oxygen Consumption.** In the absence of microbes consuming oxygen diffusing from the intestinal tissue, we hypothesized that the luminal contents itself must consume oxygen. At least two classes of abundant organic compounds can serve as substrates for oxidative reactions involving molecular oxygen and thus potentially cause oxygen consumption in the gut of germ-free animals: phospholipids and proteins. To search for lipid and protein oxidation signatures, we performed lipidomic and proteomic analyses of the cecal contents from germ-free mice in paired specimens before and after the consumption of oxygen using the in vitro model system described above (Fig. 3A).

Lipidomic analysis revealed a significant decrease in the content of several unsaturated phospholipids upon consumption of oxygen by the luminal contents from germ-free mice (Fig. 3B). As we were unable to detect any concurrent increase in the corresponding oxidation products, which could be due to the fact that these multiple products appeared as minor signals among unresolved components of complex liquid chromatography high-resolution mass spectrometry (LC-MS/MS) data, we performed the same incubations with the addition of [ $^2\text{H}_{11}$ ]-linoleic acid (LA). LA was chosen as a model lipid because it was one of the fatty acids esterified in the four most abundant lipids in previous incubations. We used a highly sensitive LC-MS/MS methodology, where the oxidation products, hydroxyoctadecadienoic acids (HODEs), are derivatized as pentafluorobenzyl esters to be good substrates for electron capture (19). Indeed, this revealed a significant increase in the concentration of [ $^2\text{H}_{11}$ ]-13-HODE after incubation that is consistent with the formation of an oxidation product from [ $^2\text{H}_{11}$ ]-LA (Fig. 3B, *Inset*). It should be noted that there is a baseline level of [ $^2\text{H}_{11}$ ]-13-HODE before incubation due to the exposure of [ $^2\text{H}_{11}$ ]-LA to atmospheric oxygen while it was being inoculated into the germ-free cecal material. Additionally, the low yield of this oxidized product after incubation is very likely due to the fact that this is just one of the many products that can be formed from LA oxidation (20). The proteomic analysis of the luminal contents proved less conclusive. Tryptic digests of cecal protein extracts were analyzed by LC-MS/MS to detect oxidation of the side chains of cysteine, methionine, tryptophan, and phenylalanine (21, 22). Little to no change was observed in the relative abundances of the quantifiable peptide-based oxidation products in the cecal contents of germ-free mice exposed to oxygen (Fig. S2).

Thus, the lipidomics results suggest that lipid oxidation by oxygen may be among the mechanisms involved in maintaining the anaerobic environment of the gut.

**Consistent with Oxygen Measurements in the Gut Lumen, Proteobacteria and Actinobacteria Are Predominant Organisms in the Mucosally Adherent and Luminal Microbiota in the Proximal Small Intestine.** The composition of the gut microbiota is highly variable along the length of the gut as well as across the intestine, and the mechanisms underlying the heterogeneity remain poorly characterized. For example, the taxa belonging to the Proteobacteria and Actinobacteria phyla are much more abundant in the small intestine than in the colon (11, 23). Similar observations have been reported for the mucosally adherent rectal microbiota relative to feces (10). In a separate group of mice from those used for our phosphorescence experiments, we have previously characterized the composition of the mucosally adherent vs. luminal microbiota along the length of the murine intestinal tract in the lumen as well as of the microbiota adherent to the mucosal surface (13). Herein, we examined the abundance of the four bacterial phyla that account for greater than 98% of the taxa: Proteobacteria, Actinobacteria, Bacteroidetes, and Firmicutes. The first two phyla are highly

enriched in aerotolerant bacteria that are either aerobes or facultative anaerobes (23).

The fractions of Bacteroidetes and Firmicutes remained relatively constant in both the luminal contents and the mucosa throughout the length of the small intestine but then diverged beginning in the cecum (Fig. 4A), where they, combined, reach the highest levels in the feces similar to previous studies (24). By contrast, the relative proportions of both the mucosally adherent and luminal Proteobacteria and Actinobacteria—the phyla that contain aerotolerant organisms—showed dramatic differences along the length of the small intestine (Fig. 4A and Fig. S3). Consistent with greater levels of luminal oxygen in the proximal small intestine, the proportions of both Actinobacteria and Proteobacteria were the highest in the proximal small intestine but decreased toward the distal gut, with the lowest levels in the proximal large intestine. Also consistent with the existence of a radial (cross-sectional) oxygen gradient in the gut (10), there were greater fractions of both Actinobacteria and Proteobacteria adherent to the mucosa than in the luminal contents of the small intestine. Indeed, the abundance of Proteobacteria in the proximal small intestine (~30%) is similar to the abundance of this phylum described in the dysbiotic fecal microbiota for inflammatory bowel disease (24–26).

The biomass of bacteria, quantified by real-time PCR of 16S rRNA gene copies, increases over 1,000-fold from the proximal small intestine to the cecum in parallel with decreasing levels of luminal oxygen (Fig. 2A) and increasing abundance of both Actinobacteria and Proteobacteria. We roughly estimated oxygen consumption by the luminal and mucosally adherent microbiota (Fig. 4C) based on the estimates of oxygen consumption by *E. coli* during log phase growth in vitro, which is  $\sim 2.4 \times 10^{-7}$  mmol  $\text{O}_2 \cdot \text{CFU}^{-1} \cdot \text{d}^{-1}$  (27), and the taxonomic assignments representing over 90% of the 16S-tagged sequences classified as

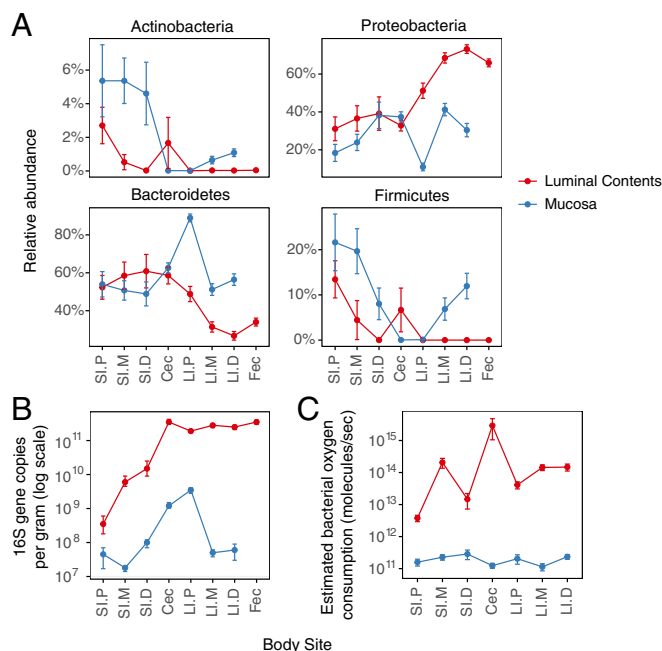


**Fig. 4.** Oxygen consumption by bacteria along the intestinal tract. (A) Proportion of the four major bacterial phyla comprising the gut microbiota in luminal and mucosal samples throughout the length of the intestinal tract, as determined by 16S rRNA gene tag sequencing. (B) Total bacterial abundance in luminal and mucosal samples, as quantified by real-time qPCR of 16S rRNA gene copies. (C) Estimated oxygen consumption rate by luminal and mucosally adherent bacteria along the intestinal tract. Cec, cecum; Fec, feces; L.I.D., large intestine–distal; L.I.M., large intestine–mid; L.I.P., large intestine–proximal; S.I.D., small intestine–distal; S.I.M., small intestine–mid; S.I.P., small intestine–proximal.

aerobes, facultative anaerobes, and obligate anaerobes as described in *SI Methods*. The data on relative abundance (Fig. 4A and Fig. S4) and 16S copy number (Fig. 4B) were used for these calculations.

The capacity of oxygen consumption by luminal gut bacteria was much greater than by the bacteria adherent to the mucosa throughout the length of the gut, which is consistent with the ability of fecal material in the cecum of conventionally housed mice to rapidly deplete oxygen *in vitro* (Fig. 3A). The estimated oxygen consumption capacity was the lowest in the proximal small intestine. In total, these results suggest that the biomass of the oxygen-tolerant bacteria in luminal contents determines the level of oxygen in the intestinal luminal environment. The low biomass in the proximal small intestine, possibly in combination with the large surface area of the villi, results in higher levels of luminal oxygen and consequently higher abundance of Proteobacteria and Actinobacteria (Fig. S5). Of course, this model assumes that the respiratory activity of bacteria in the lumen is comparable to those located on the mucosal surface, a notion that requires empirical validation.

## Discussion

Using real-time quantification of luminal oxygen concentrations throughout the length of the intestinal tract, combined with an analysis of both the composition and biomass of the gut microbiota, we provide evidence for interactions between the gut microbiota and the host tissue at the mucosal interface. The high levels of luminal oxygen in the proximal small intestine suggest that there exists a unique environment in which the gut microbiota resides. These higher oxygen levels, relative to the average  $pO_2$  in the stomach, may be due to several factors: (i) differences in the vascular perfusion of duodenal gastric tissue; (ii) greater surface area of the duodenum with its villus architecture enhancing oxygen delivery from tissue in the lumen of the gut; (iii) delivery of pancreatico-biliary secretions, which may be oxygenated, into the proximal small intestine; and (iv) the semiliquid nature of the luminal contents in the duodenum facilitating oxygen diffusion. In response, taxa belonging to both the Proteobacteria and Actinobacteria phyla exhibit the greatest abundance in the proximal intestine, with greater representation in mucosally adherent sections of the lumen (Fig. S5). The consumption of oxygen by a facultative anaerobe, such as *E. coli* K12, has been measured to range from 93,000 to 72 molecules per colony-forming unit per second in transitioning from the log to stationary phase growth. This difference reflects the metabolic capacity of bacteria dependent upon nutrient availability, where limiting levels are observed at the stationary phase (27). Since *in vitro* studies of facultative anaerobes show that oxygen has a profound effect on the bacterial metabolism (28), the presence of oxygen is likely to have a significant effect on proximal small intestinal microbiota metabolism of the nutrients delivered from the stomach.

We propose that the low bacterial biomass in the proximal small intestine is not sufficient to reduce luminal oxygen content significantly. However, the dramatic increase in the luminal bacterial biomass more distally in the gut predicts a much greater capacity for the gut microbiota to consume oxygen (Fig. 4C). Additionally, the lower surface area-to-volume ratio in the distal small intestine with shorter villi, and in the cecum/colon, where the villi are essentially absent, as well as the increasingly more solid nature of the luminal contents as they are desiccated during the transit through the length of the intestinal tract, jointly contribute to a decrease in the luminal oxygen concentration, as evidenced by our measurements. The higher fractions of Proteobacteria and Actinobacteria specifically in the mucosally adherent microbiota in the mid- and distal colon might be due to the diffusion of oxygen into the limited volume of mucus (Fig. S5). Indeed, we have previously reported higher levels of Proteobacteria and Actinobacteria in rectal biopsies and swabs, representing the mucosally adherent microbiota, relative to fecal samples (10).

Based on the above discussion, it could have been assumed that in the absence of a gut microbiota, such as in germ-free

mice, the lumen would have oxygen concentrations similar to those in the surrounding tissue. However, our measurements provide evidence to the contrary. Two possibilities are consistent with our findings. First, the intestinal tissue itself, namely the intestinal epithelium (29), may be consuming oxygen, which is initially present in the lumen (e.g., dissolved in foods), thus serving as an oxygen sink. To this end, alterations in colonic epithelial oxygen consumption may play a role in the enhanced growth of bacterial pathogens by promoting their respiration (30). Second, we provide evidence that oxidative chemical reactions in the lumen, such as lipid oxidation, are able to reduce intraluminal oxygen levels. Oxidation of phospholipids may occur by various mechanisms, including enzymatic and non-enzymatic reactions involving molecular oxygen (31). Evidence for lipid oxidation was obtained through the time-dependent reduction in concentrations of polyunsaturated phospholipids [such as phosphocholines PC(34:2), PC(34:1), PC(36:2), PC(36:3), PC(36:5)], and the addition of deuterium-labeled LA (18:2) led to an increase in the concentration of LA-specific oxidation products (13-HODE) following oxygen consumption. In contrast to lipid oxidation, the proteomics analysis in this study, which focused on specific oxidation products of cysteine, methionine, tryptophan, and phenylalanine, did not identify a major pathway of oxygen consumption by proteins in the cecal contents of germ-free mice.

Although the consumption of oxygen by chemical reactions is much slower than by bacteria, in germ-free animals, it appears to be responsible for reducing luminal oxygen levels from  $\sim 40$  mmHg to near zero over 5–6 h, as luminal contents pass through the murine intestinal tract (32). At the same time, it is likely that the diffusion rate of oxygen from the intestinal tissue into the luminal environment decreases when moving along the gut from the duodenum to the cecum (Fig. 2A). Indeed, the surface area (proportional to the presence and length of villi) of the intestine is reduced along the length of the intestinal tract (Fig. S5), and the fecal material becomes more desiccated as it traverses the gut, where its contents are liquid in the duodenum and solid in the colon (Fig. S5). The biological significance of the chemical consumption of oxygen in adult conventional animals is unlikely to be high. Nonetheless, at early stages of life, chemically created hypoxia in the lumen of the gut may play a role in the early colonization of the infant gut, where facultative anaerobic bacteria are dominant (33).

The anaerobic nature of the intestinal tract provides an explanation for observations made in germ-free mice, where obligate anaerobes can colonize the gut and demonstrate fermentative metabolism (5). Additionally, our findings may have practical implications for therapies in which fecal material is transferred from a healthy donor to a patient with disease—a practice known as fecal microbiota transplantation (FMT)—currently used primarily for the treatment of recurrent *Clostridium difficile* infection (34). The slow diffusion of oxygen into semisolid luminal material along with the ability of this material to consume oxygen may play a role in reducing the exposure of obligatory anaerobic bacterial taxa, such as *Clostridium spp.* to oxygen, as feces is processed for FMT (34), thus enhancing bacterial survival and therapeutic benefit to the recipient.

Overall, the delivery of oxygen from the host and its consumption by bacteria in the luminal environment of the intestinal tract appears to play an important role in both the composition and function of the gut microbiota. Host factors such as intestinal surface area and tissue oxygenation, combined with the physical and chemical properties of fecal material, interact in a differential fashion with the gut microbiota, leading to spatially distinct communities along both the radial and longitudinal axes of the mammalian gut.

## Materials and Methods

**Preparation and Calibration of Microsphere-Based Oxygen Probe (Oxyphor Micro5).** PMMA spheres were generated with a flow-focusing glass capillary microfluidic device according to Norton et al. (35). The diameter of the

PMMA spheres was  $\sim 32 \pm 2 \mu\text{m}$ . Oxyphor MicroS was calibrated in three viscous materials—peanut butter, vacuum grease, and hand cream—using a previously described setup (10). Additionally, each batch of Oxyphor MicroS was calibrated directly in the cecal material.

**Intraluminal and Intravascular Oxygen Measurements.** Oxyphor MicroS was fed to mice in white bread sterilized by  $\gamma$ -irradiation. For stomach and duodenum measurements, mice were fasted for 10–12 h and fed the probe followed by measurements after 90–270 min. For ileum and cecum measurements, mice were fed 12–15 h before the measurements. For intravascular measurements, Oxyphor G4 (12) (100  $\mu\text{L}$ , 200  $\mu\text{M}$  solution) was administered via a tail vein injection 10–15 min before the measurements.

Conventional C57/BL6 mice (8–12 wk of age; Jackson Laboratories) had free access to the irradiated standard chow unless otherwise specified. Germ-free C57/BL6 mice (8–12 wk of age) were provided by the University of Pennsylvania Gnotobiotic Mouse Facility. Anesthesia was induced by isoflurane inhalation (4% mixed with air). Subsequently, the isoflurane fraction was decreased to 2.5% followed by laparotomy. The mice were euthanized upon completion of the experiments. All experimental protocols were approved by the Institutional Animal Care and Use Committee at the University of Pennsylvania.

**In Vitro Oxygen Consumption Studies.** Cecal contents collected from conventionally housed or germ-free mice were weighed, dispersed in sterile water in a scintillation vial, and allowed to equilibrate with the air in the headspace under stirring for 20–30 min to re-aerate the cecal contents. The contents were then transferred to a 3-mL glass vial, and a stock solution of Oxyphor G4 (20  $\mu\text{L}$ , 200  $\mu\text{M}$ ) was then added. The vial was topped off with distilled sterile water and sealed, leaving no gaseous headspace. The contents were continuously stirred, incubated at 37  $^{\circ}\text{C}$ , and phosphorescence lifetime measurements were conducted as previously described (10). All incubations with germ-free cecal contents were run for 24 h under sterile

conditions. *E. coli* ATCC 17922 was purchased from the American Type Culture Collection and grown on Luria broth/agar. *C. sordelli* was grown on Brain Heart Infusion broth/agar. *E. coli* and *C. sordelli* were grown overnight at 37  $^{\circ}\text{C}$  under aerobic and anaerobic conditions, respectively. Cell density (colony forming units per milliliter) was measured by optical density at 630 nm, and cells were added to incubations ( $1.25\text{--}1.5 \times 10^9$  cfu/g cecal contents for *E. coli* and  $1.75\text{--}2.15$  cfu/g cecal contents for *C. sordelli*). Deuterium isotope studies were performed using 25  $\mu\text{g}$  of LA (Cayman Chemical), which was added to each incubation after aeration and mixed briefly; the first sample (before) was collected within 5 min, and the second sample (after) was obtained after incubation at 37  $^{\circ}\text{C}$  for 24 h. For lipidomic and proteomic analyses, aliquots were collected before re-aeration, after re-aeration but before incubation, and after incubation and stored at  $-80^{\circ}\text{C}$  for further use. Further information on the experimental methods involving lipidomic and proteomic analysis is available in *SI Methods*.

**16S-Tagged Sequencing and Copy Number PCR.** DNA sequence data and real-time PCR data were published previously (13). 16S rRNA marker gene sequences were analyzed with the QIIME bioinformatics software pipeline (36), using default parameters in the de novo workflow for sequence clustering and taxonomic assignment.

**ACKNOWLEDGMENTS.** This work was supported by the following: NIH Grant R01 GM103591 and NIH Human-Microbial Analytic and Repository Core of the Center for Molecular Studies in Digestive and Liver Disease Grant P30 DK 050306 (to G.D.W.); NIH Grants R01 EB018464 (to S.A.V.), R01 GM080279 (to M.G.), R24 NS092986 (to S.A.V.), and 2T32CA009140-41A1 (to P.J.L.); the PennCHOP Microbiome Program (G.D.W.); National Science Foundation Penn Materials Research Science and Engineering Center Grant DMR11-20901 and the NSF Optical Microscopy Program (to S.A.V.); and NSF Grants P42E5023720 and P30E5013508.

- Donaldson GP, Lee SM, Mazmanian SK (2016) Gut biogeography of the bacterial microbiota. *Nat Rev Microbiol* 14:20–32.
- Zhang Z, et al. (2014) Spatial heterogeneity and co-occurrence patterns of human mucosal-associated intestinal microbiota. *ISME J* 8:881–893.
- Johansson ME, Larsson JM, Hansson GC (2011) The two mucus layers of colon are organized by the MUC2 mucin, whereas the outer layer is a legislator of host-microbial interactions. *Proc Natl Acad Sci USA* 108:4659–4665.
- Swidsinski A, Loening-Baucke V, Verstraeten H, Osowska S, Doerffel Y (2008) Biostructure of fecal microbiota in healthy subjects and patients with chronic idiopathic diarrhea. *Gastroenterology* 135:568–579.
- Sonnenburg JL, et al. (2005) Glycan foraging in vivo by an intestine-adapted bacterial symbiont. *Science* 307:1955–1959.
- Salzman NH, et al. (2010) Enteric defensins are essential regulators of intestinal microbial ecology. *Nat Immunol* 11:76–83.
- Palm NW, et al. (2014) Immunoglobulin A coating identifies colitogenic bacteria in inflammatory bowel disease. *Cell* 158:1000–1010.
- Moon C, et al. (2015) Vertically transmitted faecal IgA levels determine extra-chromosomal phenotypic variation. *Nature* 521:90–93.
- Dominguez-Bello MG, Blaser MJ, Ley RE, Knight R (2011) Development of the human gastrointestinal microbiota and insights from high-throughput sequencing. *Gastroenterology* 140:1713–1719.
- Albenberg L, et al. (2014) Correlation between intraluminal oxygen gradient and radial partitioning of intestinal microbiota. *Gastroenterology* 147:1055–1063.e8.
- El Aidy S, van den Bogert B, Kleerebezem M (2015) The small intestine microbiota, nutritional modulation and relevance for health. *Curr Opin Biotechnol* 32:14–20.
- Esipova TV, et al. (2011) Two new “protected” oxyphors for biological oximetry: Properties and application in tumor imaging. *Anal Chem* 83:8756–8765.
- Liang X, et al. (2015) Bidirectional interactions between indomethacin and the murine intestinal microbiota. *eLife* 4:e08973.
- Hentati N, et al. (1999) Arterial supply of the duodenal bulb: An anatomical study. *Surg Radiol Anat* 21:159–164.
- Helander HF, Fändriks L (2014) Surface area of the digestive tract—Revisited. *Scand J Gastroenterol* 49:681–689.
- Wilson DF, Erecińska M, Drown C, Silver IA (1979) The oxygen dependence of cellular energy metabolism. *Arch Biochem Biophys* 195:485–493.
- Kawasaki S, Sakai Y, Takahashi T, Suzuki I, Niimura Y (2009) O<sub>2</sub> and reactive oxygen species detoxification complex, composed of O<sub>2</sub>-responsive NADH:rubredoxin oxidoreductase-flavoprotein A2-desulfoferrodoxin operon enzymes, rubroperoxin, and rubredoxin, in *Clostridium acetobutylicum*. *Appl Environ Microbiol* 75:1021–1029.
- Riebe O, Fischer RJ, Wampler DA, Kurtz DM, Jr, Bahl H (2009) Pathway for H<sub>2</sub>O<sub>2</sub> and O<sub>2</sub> detoxification in *Clostridium acetobutylicum*. *Microbiology* 155:16–24.
- Lee SH, Blair IA (2007) Targeted chiral lipidomics analysis by liquid chromatography electron capture atmospheric pressure chemical ionization mass spectrometry (LC-EAPCI/MS). *Methods Enzymol* 433:159–174.
- Williams MV, Lee SH, Pollack M, Blair IA (2006) Endogenous lipid hydroperoxide-mediated DNA-adduct formation in min mice. *J Biol Chem* 281:10127–10133.
- Davies MJ (2003) Singlet oxygen-mediated damage to proteins and its consequences. *Biochem Biophys Res Commun* 305:761–770.
- Davies MJ (2005) The oxidative environment and protein damage. *Biochim Biophys Acta* 1703:93–109.
- Degli Esposti M, et al. (2015) Molecular evolution of cytochrome bd oxidases across proteobacterial genomes. *Genome Biol Evol* 7:801–820.
- Peterson DA, Frank DN, Pace NR, Gordon JI (2008) Metagenomic approaches for defining the pathogenesis of inflammatory bowel diseases. *Cell Host Microbe* 3:417–427.
- Frank DN, et al. (2007) Molecular-phylogenetic characterization of microbial community imbalances in human inflammatory bowel diseases. *Proc Natl Acad Sci USA* 104:13780–13785.
- Lewis JD, et al. (2015) Inflammation, antibiotics, and diet as environmental stressors of the gut microbiome in pediatric Crohn's disease. *Cell Host Microbe* 18:489–500.
- Riedel TE, Berelson WM, Nealson KH, Finkel SE (2013) Oxygen consumption rates of bacteria under nutrient-limited conditions. *Appl Environ Microbiol* 79:4921–4931.
- Link H, Fuhrer T, Gerosa L, Zamboni N, Sauer U (2015) Real-time metabolome profiling of the metabolic switch between starvation and growth. *Nat Methods* 12:1091–1097.
- Glover LE, Lee JS, Colgan SP (2016) Oxygen metabolism and barrier regulation in the intestinal mucosa. *J Clin Invest* 126:3680–3688.
- Lopez CA, et al. (2016) Virulence factors enhance *Citrobacter rodentium* expansion through aerobic respiration. *Science* 353:1249–1253.
- Domingues MRM, Reis A, Domingues P (2008) Mass spectrometry analysis of oxidized phospholipids. *Chem Phys Lipids* 156:1–12.
- Padmanabhan P, Grosse J, Asad AB, Radda GK, Goley X (2013) Gastrointestinal transit measurements in mice with 99mTc-DTPA-labeled activated charcoal using NanoSPECT-CT. *EJNMMI Res* 3:60.
- Bäckhed F, et al. (2015) Dynamics and stabilization of the human gut microbiome during the first year of life. *Cell Host Microbe* 17:852.
- Kelly CR, et al. (2015) Update on fecal microbiota transplantation 2015: Indications, methodologies, mechanisms, and outlook. *Gastroenterology* 149:223–237.
- Norton MM, Brugarolas T, Chou J, Lee D, Bau HH (2014) Ellipsoidal particles encapsulated in droplets. *Soft Matter* 10:4840–4847.
- Caporaso JG, et al. (2010) QIIME allows analysis of high-throughput community sequencing data. *Nat Methods* 7:335–336.
- Salzman NH, et al. (2002) Analysis of 16S libraries of mouse gastrointestinal microflora reveals a large new group of mouse intestinal bacteria. *Microbiology* 148:3651–3660.
- Ormerod KL, et al. (2016) Genomic characterization of the uncultured Bacteroidales family S24-7 inhabiting the guts of homeothermic animals. *Microbiome* 4:36.
- Lagkouvardos I, et al. (2016) The Mouse Intestinal Bacterial Collection (miBC) provides host-specific insight into cultured diversity and functional potential of the gut microbiota. *Nat Microbiol* 1:16131.
- Hedlund BP, Yoon J, Kasai H (2015) *Bergey's Manual of Systematics of Archaea and Bacteria* (John Wiley & Sons, Ltd, Hoboken, NJ).
- Collins MD, et al. (1994) The phylogeny of the genus *Clostridium*: Proposal of five new genera and eleven new species combinations. *Int J Syst Bacteriol* 44:812–826.